Structure of $Li_xRb_{1-x}PO_3$ Glasses Near the Glass Transition

Andreas Hall and Jan Swenson
Department of Applied Physics, Chalmers University of Technology, S-412 96 Göteborg, Sweden

Daniel T. Bowron
Rutherford Appleton Laboratory, Chilton, Didcot OX11 0QX, UK

Stefan Adams
Department of Materials Science and Engineering, National University of Singapore, 117574, Singapore

Abstract

The temperature dependence of mixed alkali metaphosphate $Li_xRb_{1-x}PO_3$ (x=1, 0.5, 0) structures has been studied, from room temperature up to ca 20 K above the glass transition temperature (T_g), by means of neutron diffraction and reverse Monte Carlo modelling. The results show that the structural changes are limited to a slight temperature induced broadening of the peaks in *S(Q)* and a linear thermal expansion of 50-100 ppm/K. Furthermore, the possible diffusion pathways of the mobile ions have been investigated by the bond valence technique and the results show that neither these are significantly affected as the glass is brought above T_g. The decrease in activation energy that occurs above T_g is thus attributed to an increased coupling between the motions of the mobile ions and the relaxation of the phosphate network.

PACS:

1. Introduction

An important challenge in glass science in general and solid electrolytes in particular is the well-known mixed alkali effect (or more generally speaking; the mixed mobile ion effect (MMIE), since the phenomenon is not exclusively found for alkali ions). The mixed alkali effect (MAE) refers to the large changes in many dynamic properties that occur when a fraction of the mobile ions is substituted by another type of mobile ions. The largest deviations from linearity, when the concentration ratio between the two mobile ions is changed, are observed in those properties which are related to ionic transport, such as ionic conductivity, where, for instance, the here studied $Li_xRb_{1-x}PO_3$ glass system shows a drop in conductivity of about 8 orders of magnitude at room temperature for x=0.5 compared to a linear behaviour between the two single alkali glasses. Such dramatic variations of ionic transport properties may occur despite the fact that properties related to structural relaxation, such as viscosity and glass transition temperature, T_g, usually exhibit only small deviations from linearity. Similar composition dependences are furthermore observed in mixed glass-forming systems which do not contain any cations.

The MAE has been known for a long time, and extensive reviews were given by Isard [1] and Day [2] already more than 30 years ago. However, it is not until more recently a reasonable understanding of the MAE has been developed, mainly from molecular dynamics simulations and other computational techniques that have provided more detailed insight into the MAE than experimental studies alone. These computational studies suggest that an ionic jump into a

site adapted for a dissimilar ion is associated with a large energy penalty if the two types of ions have very different local environments (as is the case in the present $Li_xRb_{1-x}PO_3$ glass system due to the large size difference between Li and Rb) [3-6]. When this energy penalty is so large that jumps to dissimilar sites basically never occur this causes the A ions to effectively block the pathways for the B ions and vice versa [7-9]. However, in systems containing two types of mobile ions with similar local environments, such as in the recently investigated $Ag_xNa_{1-x}PO_3$ glass system [10], the mixed mobile ion effect is very weak due to a common cooperative hopping process where both types of mobile ions participate [11]. Thus, in such systems the energy penalty for a jump to a dissimilar site is small and consequently the two types of ions share common pathways to a large extent, rather than block each others pathways [11]. This implies that the conduction process in mixed mobile ion glasses is not universal, but depends strongly on the difference (particularly in size) between the two types of mobile ions.

Since the conduction process in mixed mobile ion glasses is strongly dependent on the energy penalty for jumps to dissimilar sites it is also expected that the conduction process is somewhat temperature dependent. The energy penalty should always be compared with the available thermal energy, because it is the ratio between the thermal energy and this energy penalty that determines the probability of an ionic jump to a dissimilar site, and thereby also the nature of the conduction process. The temperature dependence of the conduction process is also evident from the fact that the MAE (or MMIE) decreases with increasing temperature. This is a result that naturally follows from the finding that the activation energy of the Arrhenius activated conduction process is often strongly composition dependent, i.e. the drop in conductivity, compared to the corresponding single mobile ion glasses, at an intermediate composition is associated with an increase of the activation energy of the conduction process, see e.g. Ref. [12]. Hence, the higher activation energy gives a stronger temperature dependence of the conductivity in the mixed mobile ion glasses and thereby a reduced MMIE at high temperatures, provided that the temperature is within the Arrhenius activated regime, i.e. the activation energy of the conduction process is constant over the whole temperature range. This is, however, not obviously the case when the temperature has reached above the glass transition temperature T_g, where structural relaxation processes are expected to decrease the activation energy and cause more substantial changes of the conduction process. The aim of this paper has been to investigate this high temperature conductivity behaviour of the archetypal mixed alkali glass system $Li_xRb_{1-x}PO_3$. Our investigation is based on neutron diffraction experiments both below and above T_g, as well as modelling of the microscopic glass (or supercooled liquid) structure and conduction pathways by means of reverse Monte Carlo (RMC) modelling and bond valence analysis of the RMC produced structural models. The results show that the time averaged glass structure does not change significantly as the temperature is increased to ca 20 K above T_g in the investigated glasses, neither in terms of atomic pair correlations nor in the structure and volume of the mobile ion migration pathways. Within the static glass matrix approximation and the microscopic Anderson-Stuart model [Ref: O. L. Anderson and D. A. Stuart, J. Am. Ceram. Soc. 37, 573 (1954)] of ion conductivity in glasses, no change in activation energy is to be expected for the samples here investigated. Any deviation from Arrhenius behaviour must then be ascribed a change in the glass dynamics.

2. Experimental section

Glass samples of $Li_xRb_{1-x}PO_3$ with x = {1, 0.75, 0.5, 0.25 and 0}, were prepared by mixing stochiometric amounts of Li_2CO_3, Rb_2CO_3 and $(NH_4)_2HPO_4$ in alumina oxide crucibles. The mixtures were melted and allowed to react in a furnace until a clear melt was reached. The melts were left to equilibrate at a temperature of at least 850 °C for at least 1h and then poured onto a room tempered steel mould and pressed to a thickness of ca 3 mm. The produced samples were optically homogeneous, uncoloured and transparent. All compositions display high internal stress and cracks easily when handled. The $RbPO_3$ glass proved difficult to produce without any visible signs of crystallization. The samples were finally ground into fine powders and stored in a dry environment to avoid water contamination.

The glass transition temperatures were determined using a Q1000 differential scanning calorimeter (DSC) from TA Instruments. The T_g values we obtained are given in Table 1. T_g was found to vary non-linearly with composition, exhibiting a minimum at the intermediate composition. A similar compositional dependence of T_g has been found in the $Li_xNa_{(1-x)}PO_3$ system [13]. However, our $LiPO_3$ sample shows a higher T_g than obtained in previous studies [13, 14].

Neutron diffraction measurements on the x={0, 0.5 and 1} samples were conducted at the liquid and amorphous materials diffractometer, SANDALS, at ISIS, Rutherford Appleton Laboratory in UK. This instrument is optimized for light-element containing liquids and amorphous solids and was for our purposes equipped with a furnace to measure the structure factors, $S(Q)$, at two temperatures close to T_g. The glass samples were contained in cylindrical Vanadium sample cells with an inner radius of 3.8 mm, a wall thickness of 0.02 mm and a length of 65 mm. Care where taken to avoid water contamination of the samples by vacuum-drying the samples at 100º C prior to the diffraction measurements. The data were collected at 2θ angles of 3.5-40° with incident neutron wavelengths in the range of 0.05-4 Å, giving rise to a total momentum transfer (Q-range) of 0.1 – 50 $Å^{-1}$. The data were subsequently corrected for contributions from instrument, furnace, empty cell, absorption and multiple scattering and finally normalized to absolute values using a vanadium standard. For these corrections we used the program Gudrun, based upon the ATLAS package [15]. The corrected experimental $S(Q)$ for the three compositions are shown in figure 1.

3. Reverse Monte Carlo modelling

To model the glass structures we employed the Reverse Monte Carlo modelling method [16, 17]. RMC produces a structural model by a Metropolis Monte Carlo (MMC) approach, but rather than minimizing the total energy of the structure, it minimizes the difference between $S_{comp}(Q)$ of the model structure and the experimental $S_{\exp}(Q)$, χ^2, defined as

$$\chi^2 = \sum_i \sum_j \frac{\left(S_{i,\exp}(Q_j) - S_{i,comp}(Q_j)\right)^2}{\sigma_i} \qquad \text{eq. 1}$$

where i denotes an experimental data set and its corresponding value calculated for the structure model and σ_i is a fitting parameter related to the experimental errors. RMC tends to produce the most disordered structure that is consistent with the experimental input data, so in order to produce a realistic structural model it is commonly necessary to impose certain constraints on e.g. nearest neighbour distances and coordination numbers. For meta-phosphate glasses it is well established that the glass former is based on PO_4^- tetrahedra which share two of its corners, thereby forming a polymer-like 1d chain structure. The metal ions coordinate to

the non-bridging oxygens of the PO_4^- chain, thereby creating weaker ionic bonds between different parts of the covalently bonded phosphate chain. To ensure that this network is properly formed we have imposed that each phosphor atom should coordinate to four oxygens, one third of all oxygens should coordinate to two phosphor atoms (bridging oxygens, BO) and the remaining two thirds of the oxygens should coordinate to a single phosphor atom (non-bridging oxygens, NBO). To further avoid unphysical structures of overlapping atoms closest approach distances of all atomic pairs were used. These values were determined from the experimentally obtained pair correlation functions, G(r), and tabulated ionic radii. Each such start model is then fitted to the experimental neutron structure factor $S_{\exp}(Q)$ while the constraints described above were fulfilled. Once a satisfactory agreement had been obtained, a soft bond valence constraint (described in the following section) was included to ensure a realistic coordination of all atoms in the structure.

4. The Bond Valence Method

The bond valence method (BV) is a derivate of Pauling's electrostatic valence principle for stable crystalline structures [18]. Paulings concept of bond strength was modified to relate to the length of a bond [19, 20] and is today a widely used tool in crystallography to determine the plausibility of proposed crystalline structures and to localize possible sites for light atoms such as H and Li in the structure [21]. In short, the formal charge (oxidation state) of an atom is said to be balanced by coordinating atoms of opposite charge such that local charge neutrality is obtained. The bond-valence contribution from a ligand X to a central atom M is generally expressed as

$$s_{M-X} = \exp\left[\frac{R_0 - R_{M-X}}{b}\right], \qquad \text{eq. 2}$$

where R_{M-X} is the M-X distance and R_0 and b are bond valence parameters obtained from a numerical fit to atomic distances in several known crystalline structures. In traditional BV, one usually assigns the universal value b=0.37 Å. The total valence of the central atom is then the sum of contributions from all coordinating ligand atoms in the first coordination shell:

$$V_M = \sum_{\text{coord. atoms}} s_{M-X} \qquad \text{eq. 3}$$

In a stable structure, the total valence sum of each atom should be close to its ideal value V_{ideal}, equal to the absolute formal charge.

A later development of the BV method is to assess the pathways of diffusion for mobile ions in both crystalline and amorphous solids [22, 23] by assuming that the mobile ions tend to move in regions where its valence is close to its ideal value. There is however a problem inherent with the traditional summation which is only performed over the first coordination shell. For an asymmetric position in a pathway it is not always possible to uniquely determine this shell and, furthermore, it will cause discontinuities in the BV landscape. This has been addressed by introducing a summation radius (cut-off distance) within which all coordinated atoms are included in the sum [24]. Additionally, by relating the b-parameter to the softness of the bond [25, 26] a chemically more meaningful bond length - bond strength relation is obtained. With these soft bond valence parameters we have in earlier studies shown [8, 27-29] that there is a relationship between the fractional volume accessible to a mobile ion (i.e. the volume where $\Delta V=|V-V_{ideal}|<\Delta V_{max}$) that forms a percolating pathway and both the activation energy E_a and the dc conductivity σ_{dc}, given by

$$\frac{E_a}{k_B T} = A + B\sqrt[3]{F}\ , \qquad \text{eq. 4}$$

$$\log\left(\sigma_{dc} T\sqrt{m}\right) = A' + B'\sqrt[3]{F} \qquad \text{eq. 5}$$

Where A, B, A' and B' are empirical constants.

Details of BV calculations of ionic pathways are given in refs. [8, 29, 30] and references therein, but in short: Each structural model is subdivided into ca $4*10^6$ cubic volume elements of equal size, and the bond valence of a hypothetical ion M^+ placed in the centre of each volume element is calculated according to eq. 3. Elements where $\Delta V < \Delta V_{max}$ or over which there is a sign change in $V\text{-}V_{ideal}$ are labelled accessible (the latter a criteria to overcome the limited spatial resolution), whereas elements with a higher mismatch or those within the nearest neighbour distance to another cation are labelled inaccessible. Clusters of accessible elements form regions within which the energy barriers are low enough to permit diffusion of M^+ and a percolating cluster forms a dc conduction pathway of M^+.

As mentioned above, we have applied BV constraints to the RMC modelling to ensure a realistic coordination of each ion by including a penalty for each ion whose valence deviate from its ideal value. By adding the BV term

$$\chi^2_{BV} = \sum_j \frac{\left(V_{j,ideal} - Vj\right)^2}{\sigma_j} \qquad \text{eq. 6}$$

, where the sum j is over all atoms in the structure, to the total squared mismatch we can treat the BV deviation from an ideal value in the same way as deviations from any other applied constraint or experimental data. Throughout this work we have used the soft bond valence parameters from SoftBV [26]

5. Results and discussion

Figure 1 shows the corrected neutron structure factors from the two high-temperature measurements of the three glass compositions $LiPO_3$, $Li_{0.5}Rb_{0.5}PO_3$ and $RbPO_3$ along with room temperature (RT) data from an earlier investigation [31]. In the case of the $LiPO_3$ and $Li_{0.5}Rb_{0.5}PO_3$ glasses it is noticeable that the two high-T $S(Q)$ do not differ significantly from each other, despite that one of the data sets is taken below T_g and the other above. For the $RbPO_3$ sample we see Bragg-peaks appearing in the low-Q region of the data taken at 305 °C (i.e. at a temperature still below T_g) due to a partial crystallization of the sample. Above T_g the crystallization became so severe that these data could not be appropriately compared with the data at lower temperatures. However, although Bragg-peaks were observed even in the data taken at 305 °C, it is evident in Fig. 1 that the two high-T $S(Q)$ are almost identical at Q-values above 4 $Å^{-1}$. A detailed study of the structure factors of the Li-containing samples reveal that the high-T $S(Q)$ exhibit a slight broadening of the peaks and a small shift of the first diffraction peak in the x=1 and 0.5 compositions (at 1.7 and 1.1 $Å^{-1}$ respectively) towards lower Q-values with increasing T. The broadening can be assigned to the increase in thermal disorder, while the peak shift probably arises from the thermal expansion of the sample. Through the relation $r = 2\pi / Q$ the peek shift corresponds to a linear thermal expansion coefficient of ca 100 ppm/K in the single lithium composition and ca 50 ppm/K in the mixed glass. This is somewhat larger than the expected coefficients of ca 20 ppm/K at RT

found in similar glasses [32, 33], and indicates an increase in thermal expansion as we pass T_g. Hence, we see no change of the glass structure in these glasses other than a slightly increased thermal disorder and an expansion of the glass structure when the temperature passes T_g up to the temperatures we have studied. A comparison between the two near-T_g $S(Q)$:s and the RT $S(Q)$ must be done with care since the data have been taken at different instruments and also corrected with slightly different methods. Therefore, the differences observed in Fig. 1, most pronounced in the low-Q region, are likely a result of the slightly different experimental circumstances and data corrections, rather than temperature induced real structural differences. If the structure had changed substantially with increasing temperature in the glassy state, then an even larger change had been expected when the temperature had been raised above T_g into the supercooled liquid regime. Since this is clearly not the case, no substantial structural alterations are neither expected between RT and T_g.

Furthermore, figure 2 shows the partial pair correlation functions, extracted from the RMC-produced structure models of the three samples. Again there are small differences between RT and high-T data, but a small inconstancy could be expected as explained above. Between the high temperature samples however, the differences are nearly negligible. Even the partially crystallized $RbPO_3$ sample retains essentially the same pair correlations as those of the RT measurement.

To further quantify the small structural changes that occur as we move from room temperature to above T_g, as well as study what impact, if any, these have on the mobility of the Li and Rb ions, we have calculated the BV pathways of these ions in all glass compositions and for all three temperatures of each glass. The result of such calculations represents the structural changes of the glasses that are of relevance for the ionic mobility. Figure 3 shows how the $F(P_M)$ change with temperature for a range of ΔV thresholds. The differences between the RT data and the two high-T measurements are, as can be seen, miniscule throughout the shown ΔV range. The exception is $F(P_{Rb})$ in the mixed composition, where the percolation threshold at ΔV=0.2 v.u. (the sharp drop in F) at RT moves up to ca 0.4 v.u. near T_g. The presence of a percolation limit at a relatively high ΔV demonstrates how poorly this glass is adapted for Rb mobility. However, if we instead look at the total accessible volume, we see that while the values at 240 and 290 ˚C are separated from the value at RT by about 10%, there is only a minor difference between them. Hence, no large effect can be seen in the pathway volume when we pass T_g. Furthermore, the large change in percolation threshold between RT and the two high-T models is not a good indication of a large change in the structure, but rather that in the high-T models one, of a few, narrow connections between different lager parts of the Rb-pathway has been severed.

The overall small changes in $F(P_M)$ of these glasses as the temperature is increased confirm the small structural changes in these phosphate glasses. More importantly, the bond valence landscape is essentially unchanged, even as we reach a temperature above T_g. The stability of $F(P_M)$ with the small temperature-induced structural changes is not surprising. We have in an earlier study of metal-halide doped borate glasses shown that $F(P_M)$, and thereby the activation energy of conduction, is stable with regard to distortion of the glass structure, as long as the basic borate network structure is maintained [28]. Furthermore, for a range of temperatures (not exceeding T_g), 250-500 K, E_a has been shown to be constant [12], which in itself is an indication that the potential landscape of the Anderson-Stuart model [34] is essentially unchanged

This study has shown that while the structural relaxation time of the glass matrix decreases as it is heated above T_g, there is no significant change of the structure. Any deviation from an Arrhenius behaviour that most glasses follow below T_g can thus not be attributed to a change in the actual structure, at least not in the mixed $Li_{0.5}Rb_{0.5}PO_3$ system we have studied here. Instead we propose that the decrease in E_a that occurs above T_g in many glasses should be related to the faster dynamics of the glass matrix, as is described in the Dynamic structure model (DSM) [5, 35]. According to this model, the possible mobile ion sites in a mixed alkali glass can be classified in three categories; the $\overline{A}$ sites, which are energetically adapted for an *A* ion to occupy, $\overline{B}$ sites that are adapted for a *B* ion and the $\overline{C}$ site, which is an intermediate site adapted for neither *A* nor *B* ions. In the reminder of this discussion we will let A ions be the majority metal specie in the glass. While *A* ions preferentially will make successful jumps to $\overline{A}$ sites (due to a strong backward-hopping when it enters an unfavourable site) it will still visit the unlike $\overline{B}$ and $\overline{C}$ sites. On every such visit the DSM postulates that the glass matrix will relax slightly to accommodate this unlike ion. If the frequency of visits is high enough, these relaxations may turn the unlike $\overline{B}$ or $\overline{C}$ site into an $\overline{A}$ site. Likewise, an $\overline{A}$ site that has not been visited by A ions may relax to the slightly less well adapted $\overline{C}$ site (and likewise for $\overline{B}$ sites). In a pure A glass, the amount of A atoms diffusing through the network is high enough to maintain a low-energy percolating pathway of $\overline{A}$ sites. However, as B ions are introduced, they will form $\overline{B}$ sites in the $\overline{A}$ pathways in which B ions are trapped, forming a blockade in the pathway of A ions.

The relaxation time of these sites depends on the dynamics of the glass network and the dynamic coupling between the glass matrix and the mobile ions (which influence the residence times at unfavourable sites). At low temperatures the formation of new $\overline{B}$ sites is slow and the B ions are practically stationary in the glass (assuming low B-concentration). However, as temperature is increased the glass network dynamics increases along with its coupling to the motion of the mobile ions [36, 37]. This allows for a faster creation of new $\overline{B}$ sites, which, in turn, gives rise to a higher mobility of the B ions.

This "DSM behaviour" will most likely contribute to the conductivity only at temperatures significantly above T_g, where the glass matrix dynamics allow larger structural relaxations and the matrix-mobile ion coupling is significant. However, at sufficiently high temperatures the structural relaxations of the glass network cause a reduction of the blocking effect, and thereby a decrease of the activation energy for diffusion of both A and B ions in the mixed compositions. This causes the MMIE to decrease faster above T_g than what is predicted from an extrapolation of the low temperature Arrhenius dependence.

6. Conclusions

We have shown that the structures of the mixed alkali glasses $Li_XRb_{1-X}PO_3$ do not change significantly from their room temperature structures when heated slightly above T_g. The diminished MAE at elevated temperatures is ascribed to the difference in activation energy between a single and mixed alkali glasses. As the temperature is increased, the kinetic energy of mobile ions increases and thus the chance of passing an energy barrier, as described by the Anderson-Steuart model, will increase faster for the mixed compositions having higher E_a. As the temperature is elevated above T_g, no significant structural changes occur that are able to

explain any deviation from an Arrhenius behaviour of the conductivity in these glasses. The change of E_a must then be an effect of the relative change in relaxation time for the mobile ions vs. the glass matrix, leading to an increased dynamic coupling between the mobile ions and the glass matrix. The ions can therefore no longer be considered to move in a static energy landscape, as mobile ions will change the dynamics of the PO network and vice versa. Such a case is not well described by our static structural models, but is better addressed by dynamic models, such as the dynamic structure model.

Acknowledgement
This work was financially supported by the Swedish Foundation for Strategic Research.

7. References

[1] J. O. Isard, J. Non-Cryst. Solids **1**, 235 (1969).
[2] D. E. Day, J. Non-Cryst. Solids **21**, 343 (1976).
[3] T. Uchino *et al.*, J. Non-Cryst. Solids **146**, 26 (1992).
[4] M. D. Ingram, C. T. Imrie, and I. Konidakis, J. Non-Cryst. Solids **352**, 3200 (2006).
[5] A. Bunde, M. D. Ingram, and P. Maass, J. Non-Cryst. Solids **172-7**, 1222 (1994).
[6] H. Lammert, and A. Heuer, Phys. Rev. B **72**, 214202 (2005).
[7] J. Habasaki, K. L. Ngai, and Y. Hiwatari, J. Chem. Phys. **121**, 925 (2004).
[8] J. Swenson, and S. Adams, Phys. Rev. Lett. **90**, 155507 (2003).
[9] J. Habasaki, and K. L. Ngai, Phys. Chem. Chem. Phys. **9**, 4673 (2007).
[10] A. Hall *et al.*, J. Phys.: Condens. Matter **19**, 415115 (2007).
[11] A. Hall, J. Swenson, and S. Adams, Phys. Rev. Lett. (in press).
[12] C. Karlsson *et al.*, Phys. Rev. B **68**, 642021 (2003).
[13] P. F. Green, E. F. Brown, and R. K. Brow, J. Non-Cryst. Solids **255**, 87 (1999).
[14] P. J. Miller, The Journal of Chemical Physics **71**, 997 (1979).
[15] A. K. Soper, W. S. Howells, and A. C. Hannon, (Rutherford Appleton Laboratory, Appleton, 1989).
[16] R. L. McGreevy, J. Phys.: Condens. Matter **13**, R877 (2001).
[17] R. L. McGreevy, and L. Pusztai, Mol. Sim. **1**, 359 (1988).
[18] L. Pauling, JACS **51**, 1010 (1929).
[19] G. Donnay, and R. Allman, Am. Mineral. **55**, 1003 (1970).
[20] I. D. Brown, and R. D. Shannon, Acta Crystallographica, Section A **A 29**, 266 (1973).
[21] K. Waltersson, Acta Crystallogr. Sect. A **34**, 901 (1978).
[22] J. D. Garrett *et al.*, J. Solid State Chem. **42**, 183 (1982).
[23] S. Adams, and J. Maier, Solid State Ionics **105**, 67 (1998).
[24] S. F. Radaev, L. Fink, and M. Trömel, Z. Kristallogr. **S8**, 628 (1994).
[25] S. Adams, Acta Crystallogr. Sect. B **57**, 278 (2001).
[26] S. Adams, (http://kristall.uni-mki.gwdg.de/softbv/, 2004).
[27] S. Adams, and J. Swenson, Phys. Rev. Lett. **84**, 4144 (2000).
[28] A. Hall, S. Adams, and J. Swenson, Phys. Rev. B **74**, 174205 (2006).
[29] J. Swenson, and S. Adams, Phys. Rev. B **64**, 024204 (2001).
[30] A. Hall, S. Adams, and J. Swenson, J. Non-Cryst. Solids **352**, 5164 (2006).
[31] J. Swenson, L. Borjesson, and W. S. Howells, Phys. Rev. B **57**, 13514 (1998).
[32] W. D. Drotning, Int. J. Thermophys. **6**, 705 (1985).
[33] F. Muñoz *et al.*, J. Non-Cryst. Solids **347**, 153 (2004).

[34] O. L. Anderson, and D. A. Stuart, American Ceramic Society -- Journal **37**, 573 (1954).
[35] A. Bunde, M. D. Ingram, and S. Russ, Phys. Chem. Chem. Phys. **6**, 3663 (2004).
[36] C. A. Angell, Solid State Ionics **18-19**, 72 (1986).
[37] F. S. Howell *et al.*, J. Phys. Chem. **78**, 639 (1974).

Tables

Table 1

Sample	**ρ** **1/Å^3**	**T_g** **C**	**T_g litterature** **C**	**log(σ_{dc}/Scm^{-1}) at RT**
$LiPO_3$	0.08	356	333[a], 315[b]	
$Li_{0.75}Rb_{0.25}PO_3$	0.75	310		
$Li_{0.50}Rb_{0.50}PO_3$	0.67	283		
$Li_{0.25}Rb_{0.75}PO_3$	0.63	301		
$RbPO_3$	0.57	312	230[b]+	
Reference data from [a] [13]; [b] [14]; + extrapolated				

Table captions

Table 1

Summary of number density, glass transition temperature, room temperature dc conductivity and the pre-exponential factor and activation energy of the glass samples in the study.

Figures

Figure 1.

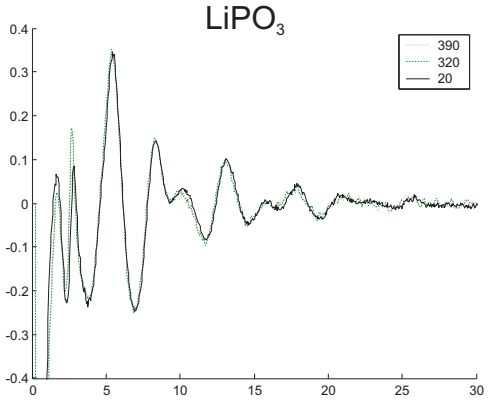

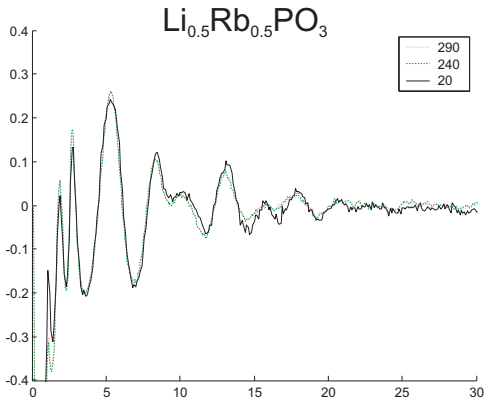

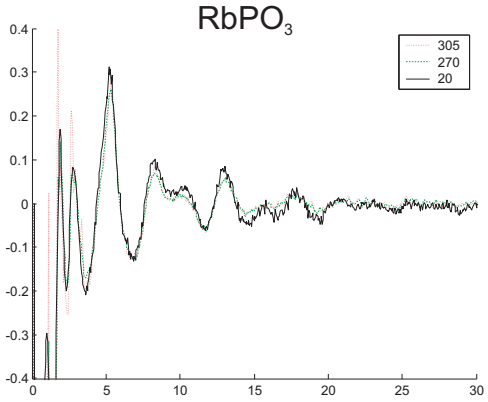

Figure 2

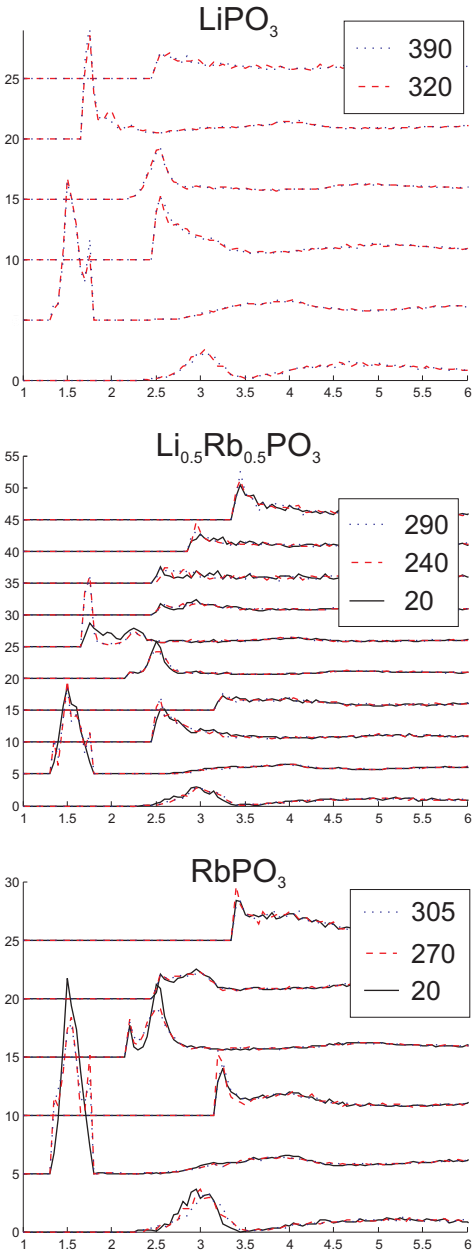

Figure3